Local Tone Mapping Using the *K*-means Algorithm and Automatic Gamma Setting

Ji Won Lee, Rae-Hong Park, *Senior Member*, *IEEE*, and SoonKeun Chang, *Member, IEEE*

Abstract—*Tone mapping (TM) algorithms reproduce the high dynamic range (HDR) images on low dynamic range (LDR) display devices such as monitors or printers. In this paper, we propose a local TM algorithm, in which the HDR input is segmented using the K-means algorithm and a display gamma parameter is set automatically for each segmented region. The proposed TM algorithm computes the luminance of an input that is the radiance map generated from a set of LDR images acquired with varying exposure settings. Then, according to the bilateral filtered luminance, an image is divided into a number of regions using the K-means algorithm. The display gamma value is set automatically according to the mean value of each region. Then, the tone of HDR image is reproduced by a local TM method with adaptive gamma value. We generate the tone-mapped image using the proposed local TM. Computer simulation with real LDR images shows the effectiveness of the proposed local TM algorithm in terms of the visual quality as well as the local contrast. It can be used for contrast and color enhancement in various display and acquisition devices.*

Index Terms—gamma setting, high dynamic range image, luminance compression, tone mapping.

I. INTRODUCTION

Tone mapping (TM) algorithm is a method that maps a real-world luminance with high dynamic range (HDR) to the luminance of the display device with limited dynamic range. That is, HDR, $[0, \infty)$, of the radiance map is mapped into a limited dynamic range, e.g., [0, 1) or [0, 255) by a TM algorithm. TM algorithm is used to compress the contrast, while preserving color ratio and details of the radiance map with the HDR. In recent years, various TM algorithms have been proposed for compressing the dynamic range of an image or video whereas retaining detail components [1, 2]. To enhance the contrast, color, and detail components, various TM algorithms have been developed, however sometimes false colors appear in the tone mapped image [3–6]. To prepare a color image for display, the dynamic range of the luminance is compressed and color correction is performed using color ratios between luminance (L) and color components (R, G, and B) of the radiance map.

TM algorithms were developed for contrast, color, and detail enhancement on display devices with a limited dynamic range. Various TM algorithms are classified into global and local methods in luminance compression. Global TM algorithms apply the same TM curve to every pixel of an image [6–14]. They are simple and fast because of using the same mapping curve for every pixel, independently of the neighboring pixels in the radiance map. They include logarithmic transformation, gamma correction, histogram equalization, and linear mapping [13]. Most global TM algorithms have nonlinear mapping functions according to the human visual system (HVS) [6–14]. Local TM algorithms [6, 15–23] use different TM curves to different regions of an image. Duan and Qui's algorithm forms a new tone reproduction curve and compresses the HDR image to enhance the local contrast [15]. iCAM algorithm, a new image appearance model, incorporates edge preserving spatial filtering with human vision photoreceptor response functions in a dual-processing framework [16]. These methods are not enough to enhance the contrast, to represent the color, and to reduce the halo effect. Also previous work produces false contours in the highlight region.

Color correction is performed by global mapping [3–7]. Previous color correction methods generate the tone mapped color image with color ratio preservation [3, 4, 5], non-linear [3, 4, 6, 19, 21] and linear [3] color saturation control. Schlick [5] presented a color correction method to preserve color ratios. Later in many TM algorithms, a nonlinear color correction function to control color saturation is used [4, 6, 19, 21]. Mantiuk *et al*. [3] proposed a linear color correction function to preserve original image colors after TM. The linear color correction method distorts hues, but better preserves luminance than the nonlinear color correction function.

The proposed TM algorithm in this paper performs the automatic color correction using a local adaptive gamma value, which is calculated by a compressed luminance of the radiance map. In the proposed TM algorithm, the luminance component of the HDR radiance map is filtered by a bilateral filter. According to the bilateral filtered luminance, an image is divided into a number of regions using the *K*-means algorithm, and then the display gamma value is determined using the mean value of each region. The proposed TM algorithm

This work was supported in part by Samsung Electronics Co., Ltd.

J. W. Lee is with the Department of Electronic Engineering, School of Engineering, Sogang University, 1 Sinsu-dong, Mapo-gu, Seoul 121-742, Korea (e-mail: nkmission@sogang.ac.kr).

R.-H. Park is with the Department of Electronic Engineering and Interdisciplinary Program of Integrated Biotechnology, Sogang University, 1 Sinsu-dong, Mapo-gu, Seoul 121-742, Korea (e-mail: rhpark@sogang.ac.kr).

S. Chang is with the Algorithm Lab., Digital Imaging Business, Samsung Electronics Co., Ltd., Suwon, Gyeonggido, 443-742, Korea (e-mail: sk107.chang@samsung.com).

Original manuscript received 01/07/11
Revised manuscript received 01/14/11
Current version published 02/21/11
Electronic version published 02/21/11.

0098 3063/11/$20.00 © 2011 IEEE

improves the local contrast and suppresses artifacts such as halo artifact, false color, and false contour. Display gamma values for TM curve are selected automatically by considering the mean values of local regions.

The rest of the paper is organized as follows. Section II proposes a TM algorithm using the *K*-means algorithm, in which an image is split into *K* clusters depending on the bilateral filtered luminance. Experimental results with three sets of low dynamic range (LDR) images are presented in Section III, showing the effectiveness of the proposed TM algorithm. Finally, Section IV concludes the paper.

II. Proposed Algorithm

The proposed TM algorithm constructs the tone-mapped image from the input, which is a HDR radiance map. To generate the HDR radiance map, we employ Debevec and Malik's algorithm [24] and use three LDR images with different exposures.

Fig. 1 shows the block diagram of the proposed TM algorithm. The input, HDR radiance map, C_{in} is generated using three LDR images of under-, mid-, and over-exposures. Also the HDR radiance map C_{in} is used for local TM in the automatic tone compression block. Each block is described in following subsections.

A. Initial grouping

Fig. 2 shows the procedure of the proposed TM algorithm using Carnival LDR images. Fig. 2(a) shows three LDR images of under-, mid-, and over-exposures (exposure time: 1/45 s, 1/2 s, and 1/3 s, aperture: f/6, ISO: 400, size: 3072×2048), where an LDR image of mid-exposure is a reference LDR image. Fig. 2(b) illustrates the luminance of an input and its histogram. Luminance of the HDR input is represented by floating-point values.

In the proposed TM algorithm, the luminance component of the HDR radiance map is filtered by a bilateral filter [20, 25] and then is mapped by a logarithmic function as an initial global mapping. For edge-preserving smoothing, a bilateral filter considers not only geometric proximity between neighboring pixels in the spatial domain, but also intensity similarity in the intensity domain [25]. Bilateral filtered luminance $\tilde{L}$ is defined as

$$\tilde{L}(p)=\frac{1}{k(p)}\sum_{q\in\Omega}G_{\sigma_s}(p-q)\,G_{\sigma_r}(L_{in}(p)-L_{in}(q))L_{in}(q) \tag{1}$$

where L_{in} denotes the luminance of an input, G represents a Gaussian function, Ω signifies the set of neighboring pixels whose center pixel is at p, and the subscripts σ_s and σ_r denote standard deviations of Gaussian weight functions in the spatial domain and intensity domain, respectively. The normalization term $k(p)$ is defined as

$$k(p)=\sum_{q\in\Omega}G_{\sigma_s}(p-q)\,G_{\sigma_r}(L_{in}(p)-L_{in}(q)). \tag{2}$$

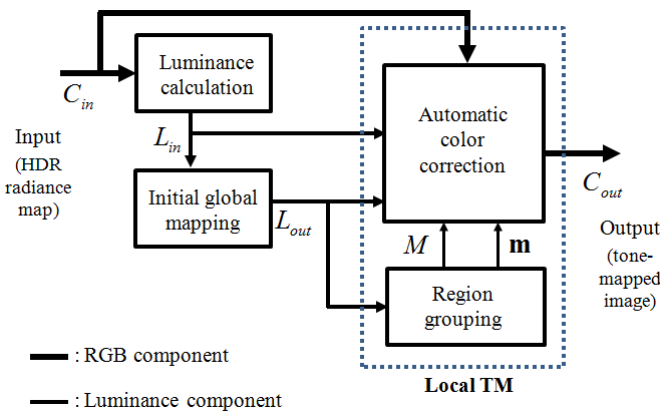

Fig. 1. Block diagram of the proposed TM algorithm.

A bilateral filter is an edge-preserving smoothing filter. Fig. 2(c) shows the bilateral filtered luminance of an input and its histogram. σ_s and σ_r are set to 2 and 80 in experiments, respectively. The histogram of the bilateral filtered luminance (Fig. 2(c)) is more stretched than that of the luminance without bilateral filtering (Fig. 2(b)). That is, bilateral filtering has the effect that the histogram is stretched while edges are preserved.

First of all, the proposed TM algorithm uses a simple global TM for global contrast enhancement, and then the local TM is used. Initial global mapping of the bilateral filtered luminance is performed by

$$L_{out}(p)=\log\left(\tilde{L}(q)\right) \tag{3}$$

where log(·) represents a logarithmic function which is used to approximate the non-linear global tone mapping considering the HVS. A logarithmic function is used in various retinex algorithms [26, 27]. It was proposed in order to enhance the global contrast of the filtered luminance in initial global mapping. Initial global mapping using a logarithmic function compresses the filtered luminance by a non-uniform mapping curve. Its input-output characteristic shows that the mapping values (filtered luminance in Fig. 2(c)) are densely distributed in the range of small luminance values and coarsely distributed in the other range. Fig. 2(d) shows the luminance of initial global mapping L_{out} and its histogram. However, the luminance of initial global mapping L_{out} is not sufficient to effectively represent the local contrast of the tone mapped image.

B. Region grouping using the K-means algorithm

In the proposed TM algorithm, the input of the *K*-means clustering block is the luminance of initial global mapping. The mapping from the luminance of the real world scene with HDR to the luminance of a device with a limited dynamic range is applied adaptively to each local region. The proposed local TM algorithm segments an image into a number of local regions according to the luminance of initial global mapping.

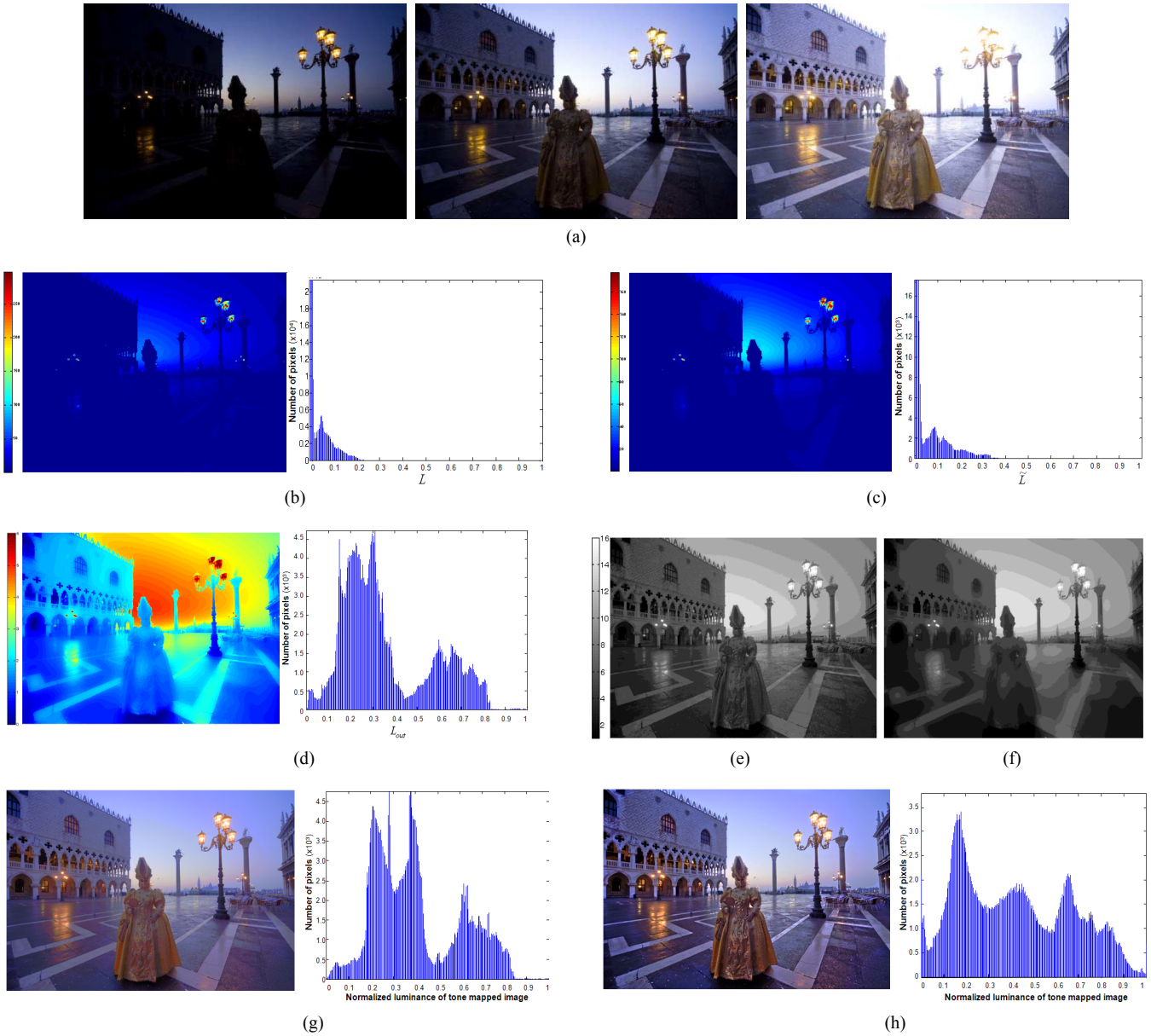

Fig. 2. Procedure of the proposed TM algorithm (Carnival LDR images, K=16, a=0.3, and γ_{max}=2.2). (a) LDR images (under-, mid-, and over-exposures: 1/45 s, 1/10 s, and 1/3 s), (b) luminance of the input L and its histogram, (c) luminance of the input (with bilateral filtering) $\tilde{L}$ and its histogram, (d) luminance of the initial global mapping L_{out} and its histogram, (e) clustering result (without bilateral filtering), (f) clustering result (initial global mapping with bilateral filtering), (g) tone-mapped image (initial global mapping without bilateral filtering) and its luminance histogram, (h) tone-mapped image (with bilateral filtering) and its luminance histogram.

Figs. 2(e) and 2(f) show the clustering results without and with bilateral filtering, respectively. Fig. 2(e) illustrates the segmented regions that have many isolated pixels, where the number of regions K is set to 16. Fig. 2(f) shows the clustering result with K equal to 16 and with bilateral filtering, in which isolated pixels are removed and the contrast of a bilateral filtered luminance is increased.

In the K-means clustering block, using the conventional K-means algorithm [28, 29] we segment an image into K cluster regions according to the luminance of initial global mapping L_{out}. The K-means algorithm assigns each pixel to the cluster whose centroid is the mean of all pixels contained in the cluster. In the proposed algorithm, let m_k be a mean value of k^{th} cluster. The mean vector $\mathbf{m}$ of K clusters is defined as

$$\mathbf{m} = [m_1, \cdots, m_k, \cdots, m_K]^T, \tag{4}$$

and the segmented region is labeled as

$$M(p) = k, \quad 1 \le k \le K. \tag{5}$$

Fig. 2(g) shows the tone-mapped image without bilateral filtering and its histogram whereas Fig. 2(h) illustrates that with bilateral filtering and its histogram. The tone-mapped

Fig. 3. Tone-mapped images with different gamma values (Carnival LDR images, a = 0.3, K = 16). (a) γ = 0.3, (b) γ = 1.0, (c) γ = 2.2.

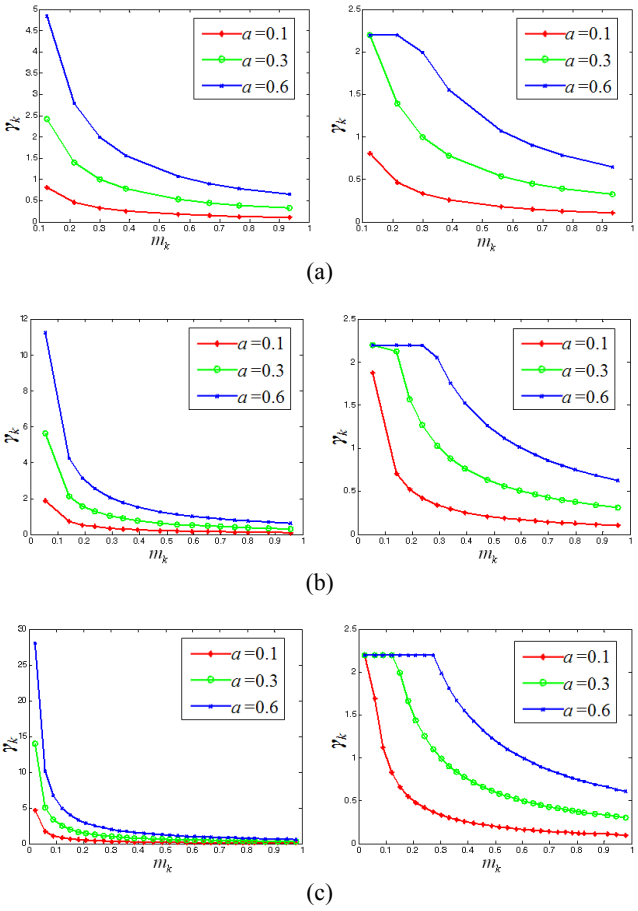

Fig. 4. Automatic gamma setting (Carnival LDR images, left: without γ_{max} setting, right: with γ_{max} = 2.2 setting). (a) K=8, (b) K=16, (c) K=32.

image in Fig. 2(g) is muddy and has a narrower dynamic range than that in Fig. 2(h).

C. Local TM and automatic gamma setting

Fig. 3 shows the tone-mapped images according to the display gamma value γ, where the same gamma value is applied to all pixels in the image. Figs. 3(a), 3(b), and 3(c) are the tone-mapped images (left) and enlarged regions (center: streetlight/building, right: sky/face) with γ = 0.3, 1.0, and 2.2, respectively, in which red boxes in Fig. 3(b) represent two enlarged regions. In the brightest (over-saturated) region such as streetlights (center) and sky (right), the color and contrast of the tone-mapped images with $\gamma \le 1.0$ look natural whereas those with $\gamma > 1.0$ are unnatural. Worst of all, false contours in the sky and the overshoot around the mask are generated with large γ in Fig. 3(c). Whereas in the dark (under-saturated) region such as the inside of the building (center), the color and detail components are rendered well in the tone-mapped image with $\gamma \ge 1.0$, as shown in Fig. 3(c). The contrast enhancement of the dark region is not enough, and the gamma value is very low to render the color value in Fig. 3(a).

In the proposed TM algorithm, the mean vector **m** of K clusters is used in automatic setting of gamma values for color correction. That is, the proposed TM algorithm generates the color tone-mapped image using the gamma value determined by considering the luminance of initial global mapping. The gamma value γ_k, where the subscript k denotes label of k^{th} cluster, is computed as

$$\gamma_k = \frac{a}{m_k} \tag{6}$$

by considering the luminance of initial global mapping, where a is a scale constant, $0 \le a \le 1$, and m_k is a mean of k^{th} cluster, $1 \le k \le K$. The gamma value γ_k is determined in proportion to scale constant a whereas in inverse proportion to the local mean m_k of k^{th} cluster.

The proposed TM algorithm limits the gamma value to a fixed maximum value. That is, automatic gamma value selected is expressed as

$$\gamma_k = \min\left\{\gamma_{\max}, \frac{a}{m_k}\right\} \tag{7}$$

where γ_{max} is the maximum gamma, $0 \le \gamma_k \le \gamma_{\max}$. The gamma vector $\boldsymbol{\gamma}$ of K clusters is defined as

$$\boldsymbol{\gamma} = [\gamma_1, \cdots, \gamma_k, \cdots, \gamma_K]^T. \tag{8}$$

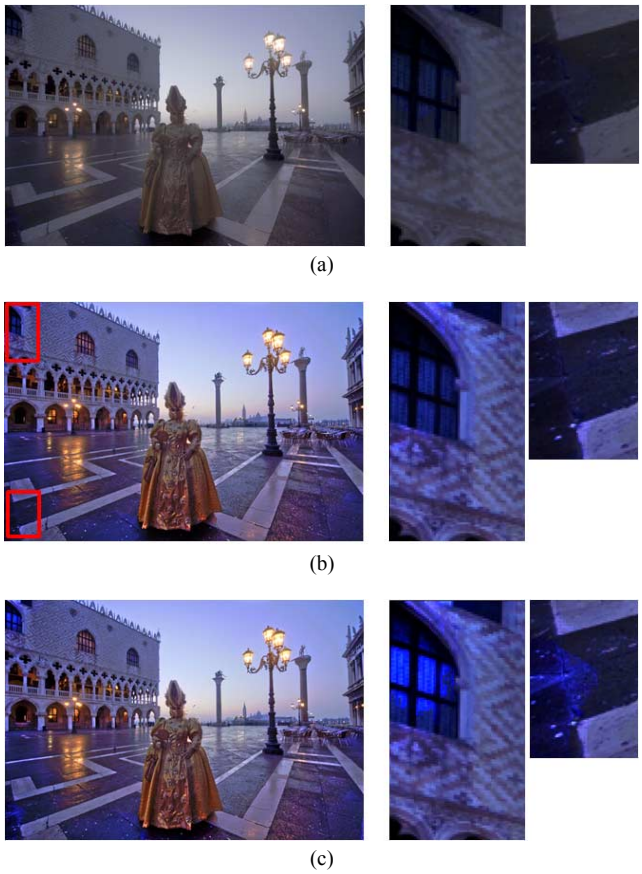

Fig. 5. Tone-mapped images with different γ_{max} values (Carnival LDR images, a = 0.3, K = 16). (a) γ_{max} = 1.8, (b) γ_{max} = 2.2, (c) γ_{max} = 4.0.

Fig. 4 shows the automatic gamma setting with different scale constant a using three Carnival LDR images. Figs. 4(a), 4(b), and 4(c) are gamma values as a function of local luminance mean, which is calculated by eqs. (6) and (7) with K = 8, 16, and 32 clusters, respectively. The input of the K-means clustering block, the luminance of initial global mapping L_{out}, is adjusted to be normalized (L_{out} = 1 for maximum luminance) and to quantize the bilateral filtered luminance $\widetilde{L}$ into a finite number of levels, which is set to 256 in experiments. As K increases, the gamma value is increased excessively, i.e., eq. (6) gives a large gamma value if the mean value of cluster is very small for large K cases.

The intensity range is limited by the maximum gamma value γ_{max} = 2.2, because the gamma value is very high in the low luminance range and an excessive large gamma value causes artifacts such as false contour and false color. Fig. 5 illustrates the effect of a different maximum gamma value γ_{max} in tone-mapped images with a = 0.3 and K = 16 using three Carnival LDR images. Figs. 5(a), 5(b), and 5(c) are tone-mapped images (left) and their enlarged regions (center: wall, right: street) with γ_{max} = 1.8, 2.2, and 4.0, respectively, in which red boxes in Fig. 5(b) represent two enlarged regions. In Fig. 5(c) with γ_{max} = 4.0, false color appears in the dark region, because the excessive gamma value is computed by the small mean value in the dark region as shown in enlarged regions. In this paper, we use the fixed maximum gamma

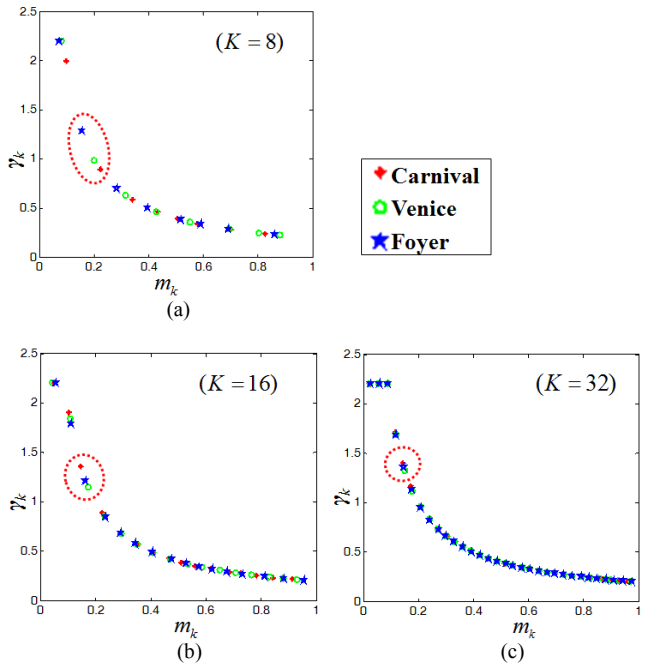

Fig. 6. Automatic gamma setting of three LDR image sets (a=0.3, γ_{max} = 2.2). (a) K=8, (b) K=16, (c) K=32.

value γ_{max} = 2.2, and the gamma value larger than γ_{max} = 2.2 causes the false color as shown in Fig. 5(c).

Fig. 6 illustrates the automatic gamma setting of three test LDR image sets (Carnival, Venice, and Foyer) with different numbers of clusters K, a = 0.3, and γ_{max} = 2.2. Figs. 6(a), 6(b), and 6(c) show the display gamma values, as a function of the luminance mean of clusters m_k with K = 8, 16, and 32, respectively. As shown in Fig. 6, the local mean m_k and thus gamma value γ_k vary with different LDR image sets. The red dotted ellipses show the gamma values of the 2nd (Fig. 6(a)), 3rd (Fig. 6(b)), and 5th (Fig. 6(c)) clusters, respectively, of three LDR image sets. The difference of gamma values in the same cluster decreases as the number of clusters K increases. In Fig. 6(c), gamma values of three LDR image sets do not differ much. That is, when the number of clusters is increased, we can use the fixed gamma values for local TM regardless of the input LDR image set, with the computation time increased. We use K=16 in experiments by considering the tradeoff between the computation time and the naturalness of color reproduction of the tone-mapped color image.

Fig. 7 shows tone-mapped images with different scale constant a. Figs. 7(a), 7(b), and 7(c) illustrate the tone-mapped images (left) and their enlarged regions (center: sky/face, right: streetlight/street) with a = 0.1, 0.3, and 1.0, respectively, in which red boxes in Fig. 7(b) represent two enlarged regions. Fig. 7(a) shows the low contrast and muddy tone-mapped image with a = 0.1, while Fig. 7(c) shows that with excessive contrast and artifacts in the brightest regions (center and right sides). We experimentally set a to 0.3.

In the proposed TM algorithm, we use the automatic gamma setting for color correction. The used gamma values in automatic color correction block are calculated by considering the statistical characteristics of local regions that are

(a)

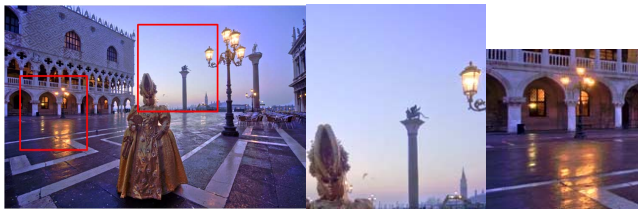

(b)

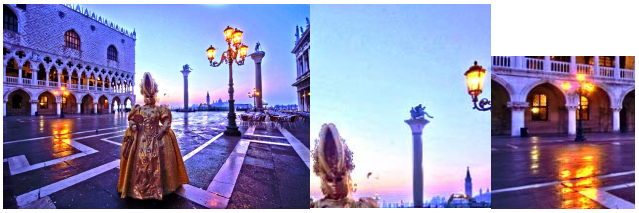

(c)

Fig. 7. Tone-mapped images with different a values (Carnival LDR images, $K = 16$, $\gamma_{max} = 2.2$). (a) $a = 0.1$, (b) $a = 0.3$, (c) $a = 1.0$.

segmented in K-means clustering block. That is, the gamma value is adaptively determined in each local region. The nonlinear color correction function [6, 19, 21] is defined by

$$C_{out}(p) = \left(\frac{C_{in}(p)}{L_{in}(p)}\right)^{\gamma} L_{out}(p) \tag{9}$$

where γ controls the color saturation and L_{out} represents the luminance after initial global mapping. The defect of the nonlinear color correction function using eq. (9) is that the luminance changes in the over-saturated regions give an undesirable side effect [3]. That is, the luminance of the tone-mapped image is changed if $\gamma \neq 1$ or $t_R R_{out} + t_G G_{out} + t_B B_{out} \neq L_{out}$ (t_R, t_G, and t_B are constants). Eq. (9) is modified as

$$\frac{C_{out}(p)}{L_{out}(p)} = f\left(\frac{C_{in}(p)}{L_{in}(p)}\right) = \left(\frac{C_{in}(p)}{L_{in}(p)}\right)^{\gamma}. \tag{10}$$

First-order Taylor series expansion of eq. (10) at $C_{in}(p)/L_{in}(p) = 1$ gives

$$\frac{C_{out}(p)}{L_{out}(p)} = f(1) + \gamma\left(\frac{C_{in}(p)}{L_{in}(p)} - 1\right) = \gamma\left(\frac{C_{in}(p)}{L_{in}(p)} - 1\right) + 1. \tag{11}$$

The linear color correction function preserves the luminance and decreases the computation time. We use the linear color correction function with local adaptive gamma values.

(a)

(b)

(c)

Fig. 8. LDR image sets used in experiments. (a) Venice (1/750 s, 1/180 s, 1/45 s), (b) Foyer (1/100 s, 1/30 s, 1/10 s), (c) Warehouse (1/4000 s, 1/1500 s, 1/350 s).

III. Experimental Results and Discussions

We use three LDR image sets to show the effectiveness of the proposed TM algorithm. Fig. 8 shows the LDR image sets used in experiments. In Fig. 8, red boxes (center) represent two enlarged regions. Fig. 8(a) shows three Venice LDR images with under-, mid-, and over-exposures (exposure time from left to right: 1/750 s, 1/180 s, and 1/45 s, aperture: f/6.7, ISO: 100, size: 1752×1168). Fig. 8(b) illustrates three Foyer LDR images with under-, mid-, and over-exposures (exposure time from left to right: 1/100 s, 1/30 s, and 1/10 s, aperture: f/8, ISO: 100, size: 1200×798). Fig. 8(c) shows three Warehouse images with under-, mid-, and over-exposures (exposure time from left to right: 1/4000 s, 1/1500 s, 1/350 s, aperture: f/2, ISO: 100, size: 2336×1552). LDR images with the mid-exposure are selected as reference LDR images in Fig. 8. In Fig. 8, LDR images are low contrast images that contain poorly exposed dark and bright regions with the narrow dynamic range. The HDR radiance map is generated by combining three LDR images of the same scene but with under-, mid-, and over-exposures.

Experimental results of five TM algorithms are shown: logarithmic transformation [13], Reinhard *et al.*'s algorithm [14], Duan and Qui's algorithm [15], iCAM algorithm [16], and the proposed method.

Fig. 9 compares the tone-mapped images (top) and their enlarged regions (bottom left (region A): sky/building, bottom right (region B): yacht/building) of Fig. 8(a), which are generated by four conventional algorithms and the proposed TM algorithm. Fig. 9(a) shows a reference LDR image, which is a mid-exposure and low-contrast image (Venice). LDR images of under-, mid-, over-exposure in Fig. 8(a) were taken in sunset. The buildings of both sides are dark in LDR images of under- and mid-exposure images in the enlarged regions A and B of Fig. 8(a), and the sky region is saturated in the over-

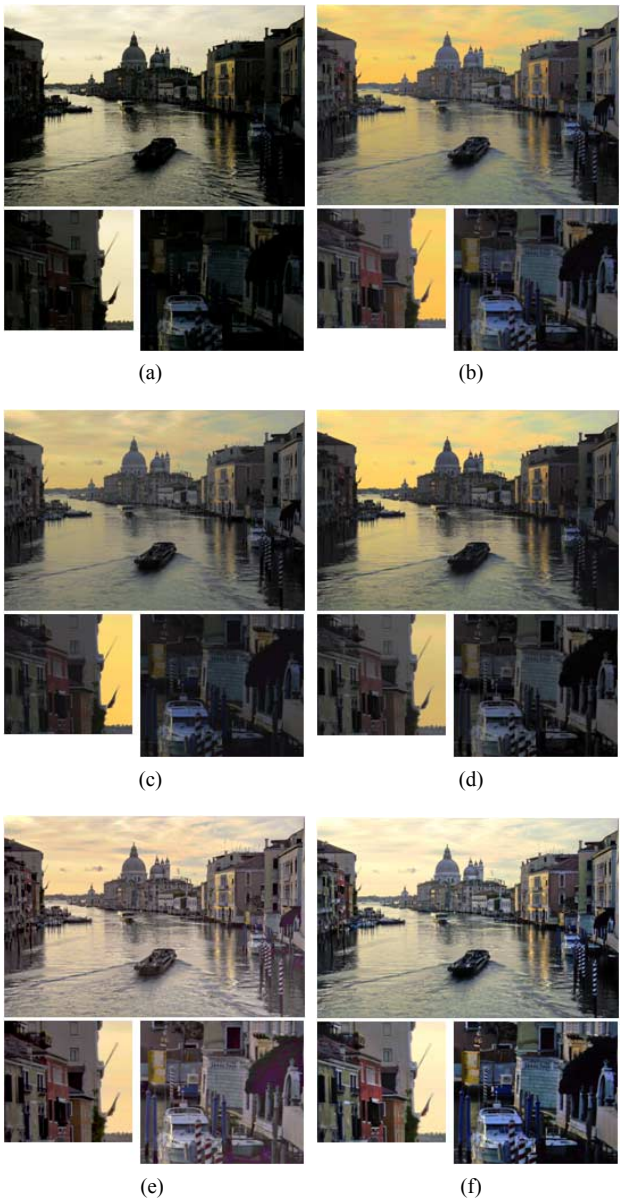

Fig. 9. Tone-mapped images (Venice). (a) reference LDR image, (b) logarithmic transformation, (c) Reinhard *et al.*'s algorithm, (d) Duan and Qui's algorithm, (e) iCAM algorithm, (f) proposed algorithm.

exposed image. Fig. 9(b) illustrates the tone-mapped image by a logarithmic transformation, in which false contours and undesired color change appear in the sky. The enlarged regions A and B are dark due to insufficient contrast enhancement. Figs. 9(c) and 9(d) show the tone-mapped images by Reinhard *et al*.'s and Duan and Qui's algorithms, respectively, in which the color of sky is better than that in Fig. 9(b), yet the contrast is not enough. Fig. 9(e) shows the tone-mapped image by the iCAM algorithm, in which the contrast is high and the detail is preserved in the sky region, however the false color appears in the enlarged region A. Fig. 9(f) illustrates the tone-mapped image by the proposed TM algorithm, in which the color is natural and contrast is high. The false color in the enlarged region A disappears and color is reconstructed well in the enlarged region B.

Fig. 10. Tone-mapped images (Foyer). (a) reference LDR image, (b) logarithmic transformation, (c) Reinhard *et al.*'s algorithm, (d) Duan and Qui's algorithm, (e) iCAM algorithm, (f) proposed algorithm.

Fig. 10 compares the tone-mapped images (top) and their enlarged regions (bottom left (region A): outside of window/round table, bottom right (region B): plants/desk lamp) of Fig. 8(b), which are reconstructed from the four conventional algorithms and the proposed TM algorithm. Both the outside and indoor are shown, however outside is clear whereas the indoor is dark because there is no light in a room in LDR images of under- and mid-exposures in Fig. 8(b). In other words, the view of the outside is saturated because the

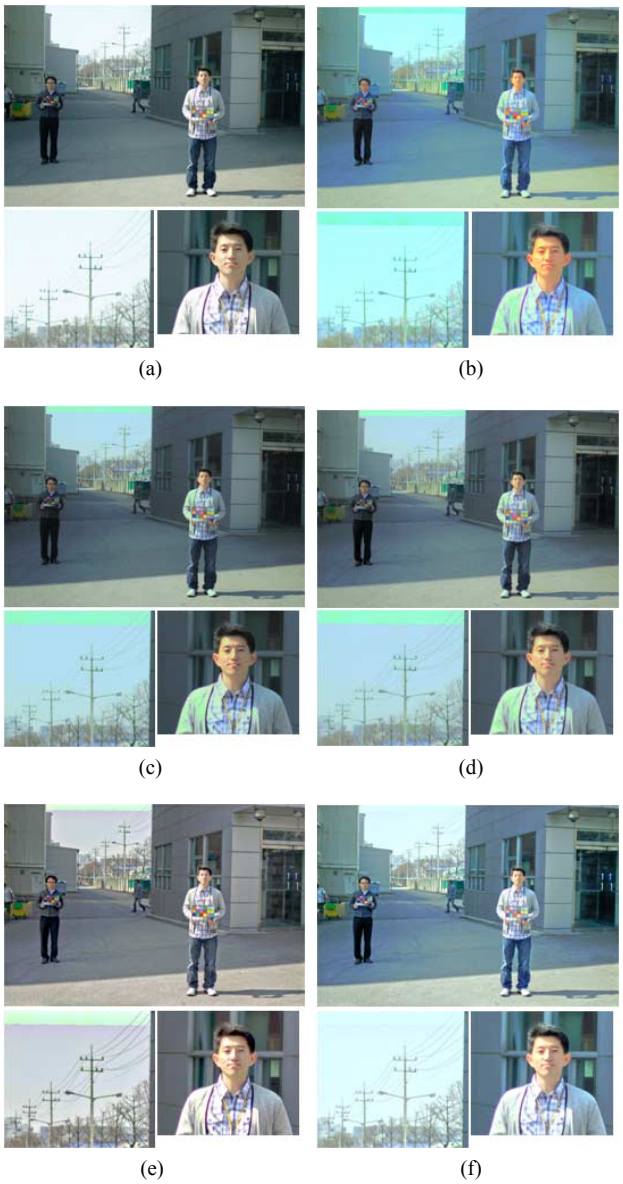

Fig. 11. Tone-mapped images (Warehouse, with alignment). (a) reference LDR image, (b) logarithmic transformation, (c) Reinhard *et al.*'s algorithm, (d) Duan and Qui's algorithm, (e) iCAM algorithm, (f) proposed algorithm.

light is outside and indoor objects look natural in a LDR image of over-exposure in Fig. 8(b). Fig. 10(a) shows a reference LDR image, which is a mid-exposure and low-contrast image (Foyer). Fig. 10(b) shows the tone-mapped image by a logarithmic transformation, in which the undesired color change appears. Figs. 10(c) and 10(d) show the tone-mapped images by Reinhard *et al.*'s and Duan and Qui's algorithms, respectively, in which the color is more natural than that in Fig. 10(b). Yet the contrast is not enough. Fig. 10(e) illustrates the tone-mapped image by iCAM algorithm, in which contrast of the outside is high, whereas that of the inside is low. Fig. 10(f) shows the tone-mapped image by the proposed TM algorithm, in which a view of the outside is of high contrast, as well as the color of indoor objects such as a glass table and flowers is vivid (enlarged region A). In Fig. 10(f), the proposed TM algorithm renders color of the desk lamps in both sides better than other algorithms (enlarged region B).

Fig. 11(a) shows the mid-exposure LDR image (top) and their enlarged regions (bottom left (region A): sky, bottom right (region B): face) in Fig. 8(c). LDR images in Fig. 8(c) have global and local motion. To generate the radiance map without ghost artifacts, we use Min *et al.*'s algorithm [30] in experiments. Regions A and B are over-saturated regions in over-exposure LDR image. In these regions of the tone-mapped image, the artifacts are generated due to wrong radiance value in over saturated region. Figs. 11(b), 11(c), 11(d), and 11(e) show tone-mapped images by a logarithmic transformation, Reinhard *et al.*'s, Duan and Qui's, and iCAM algorithms, respectively. In Figs. 11(b), 11(c), and 11(d), false colors are generated. False contours appear in the face of region B of Fig. 11(d). Fig. 11(f) illustrates the tone-mapped image by the proposed TM algorithm, in which the color is natural and contrast is high. The false color in the enlarged region A disappears and skin color is reconstructed well in the enlarged region B.

In summary, experiments with several test LDR image sets show that the proposed TM algorithm reproduces better color of the tone-mapped image than conventional TM algorithms in highlight regions. It is because of the fact that, the gamma value used in color correction of the proposed TM algorithm is selected adaptively by considering the statistical characteristics of local regions that are segmented by the *K*-means clustering algorithm.

IV. CONCLUSIONS

This paper proposes a local TM algorithm using the *K*-means algorithm and automatic gamma setting. The proposed TM algorithm consists of initial global mapping, region grouping, and automatic color correction. The region grouping using the *K*-means algorithm divides the bilateral filtered luminance into *K* clusters, and produces *K* clusters and their means, which are used for gamma setting of local TM in the automatic color correction block. The tone-mapped color image of the proposed TM algorithm gives better image quality than that of the conventional TM algorithms. That is, the proposed algorithm effectively enhances the local contrast and color with automatic gamma values selected by considering the statistical characteristics of local regions that are segmented by the *K*-means algorithm. Experimental results with three sets of LDR images show that the proposed TM algorithm efficiently enhances the local contrast of the LDR images and renders color naturally. It can be used as a post-processing for contrast enhancement in display devices. Further research will focus on improvement of the luminance compression and details enhancement. Also the color appearance in the TM will be considered for improving color in the tone-mapped color image.

REFERENCES

[1] S. Battiato, A. Castorina, and M. Mancuso, "High dynamic range imaging for digital still camera: An overview," *J. Electronic Imaging*, vol. 12, no. 3, pp. 459–469, July 2003.

[2] E. A. Khan, A. O. Akyuz, and E. Reinhard, "Robust generation of high dynamic range images," in *Proc. Int. Conf. Image Processing*, pp. 2005–2008, Atlanta, GA, Oct. 2006.

[3] R. Mantiuk, R. Mantiuk, A. Tomaszewska, and W. Heidrich, "Color correction for tone mapping," in *Proc. Eurographics 2009*, vol. 28, no. 2, pp. 193–202, Munchen, Germany, Mar./Apr. 2009.

[4] A. O. Akyüz and E. Reinhard, "Color appearance in high-dynamic-range imaging," *J. Electronic Imaging*, vol. 15, no. 3, pp. 033001-1–033001-12, July/Sept. 2006.

[5] C. Schlick, "Quantization techniques for the visualization of high dynamic range pictures," in *Proc. Photorealistic Rendering Techniques Eurographics*, pp. 7–20, Darmstadt, Germany, June 1994.

[6] J. Tumblin and G. Turk, "Low curvature image simplifiers (LCIS): A boundary hierarchy for detail-preserving contrast reduction," in *Proc. ACM SIGGRAPH2000*, pp. 83–90, New Orleans, LA, July 2000.

[7] G. J. Ward, "The radiance lighting simulation and rendering system," in *Proc. ACM SIGGRAPH94*, pp. 459–472, Orlando, FL, July 1994.

[8] G. W. Larson, H. Rushmeier, and C. Piatko, "A visibility matching tone reproduction operator for high dynamic range scenes," *IEEE Trans. Visualization and Computer Graphics*, vol. 3, no. 4, pp. 291–306, Oct./Dec. 1997.

[9] S. Nayar and T. Mitsunaga, "High dynamic range imaging: Spatially varying pixel exposure," in *Proc. IEEE Int. Conf. Computer Vision and Pattern Recognition*, vol. 1, pp. 472−479, Vancouver, Canada, June 2000.

[10] J. Cohen, C. Tchou, T. Hawkins, and P. Debevec, "Real-time high dynamic range texture mapping," in *Proc. 12th Eurographics Workshop on Rendering*, pp. 313–320, London, UK, June 2001.

[11] N. S. Pattanaik, J. Tumblin, H. Yee, and D. P. Greenberg, "Time-dependent visual adaptation for realistic image display," in *Proc. ACM SIGGRAPH2000*, pp. 47–54, New Orleans, LA, July 2000.

[12] A. Scheel, M. Stamminger, and H.-P. Seidel, "Tone reproduction for interactive walkthroughs," *Computer Graphics Forum*, vol. 19, no. 3, pp. 301–312, Aug. 2000.

[13] R. C. Gonzalez and R. E. Woods, *Digital Image Processing.* Third ed., Upper Saddle River, NJ: Pearson Education, Inc., 2010.

[14] E. Reinhard, M. Stark, P. Shirley, and J. Ferwerda, "Photographic tone reproduction for digital images," *ACM Trans. Graphics*, vol. 21, no. 3, pp. 267−276, July 2002.

[15] J. Duan and G. Qui, "Fast tone mapping for high dynamic range images," in *Proc. 17th Int. Conf. Pattern Recognition*, vol. 2, pp. 847–850, Bristol, UK, Aug. 2004.

[16] J. Kuang, G. M. Johnson, and M. D. Fairchild, "iCAM06: A refined image appearance model for HDR image rendering," *J. Vis. Commun. Image Representaion*, vol. 18, no. 5, pp. 406–414, Oct. 2007.

[17] M. Ashikhmin, "A tone mapping algorithm for high contrast images," in *Proc. 13th Eurographics Workshop Rendering*, pp. 145−155, Pisa, Italy, June 2002.

[18] E. Reinhard and K. Devlin, "Dynamic range reduction inspired by photoreceptor physiology," *IEEE Trans. Visualization and Computer Graphics*, vol. 11, no. 1, pp. 13−24, Jan. 2005.

[19] R. Fattal, D. Lischinski, and M. Werman, "Gradient domain high dynamic range compression," *ACM Trans. Graphics*, vol. 21, no. 3, pp. 249–256, July 2002.

[20] F. Durand and J. Dorsey, "Fast bilateral filtering for the display of HDR images," *ACM Trans. Graphics*, vol. 21, no. 3, pp. 257−266, July 2002.

[21] Y. Li, L. Sharan, and E. H. Adelson, "Compressing and companding high dynamic range images with subband architectures," *ACM Trans. Graphics*, vol. 24, no. 3, pp. 836–844, July 2005.

[22] Y. Monobe, H. Yamashita, T. Kurosawa, and H. Kotera, "Dynamic range compression preserving local image contrast for digital video camera," *IEEE Trans. Consumer Electronics*, vol. 51, no. 1, pp. 1–10, Feb. 2005.

[23] J. W. Lee, R.-H. Park, and S. Chang, "Tone mapping using color correction function and image decomposition in high dynamic range imaging," *IEEE Trans. Consumer Electronics*, vol. 56, no. 4, pp. 2756-2762, Nov. 2010.

[24] P. E. Debevec and J. Malik, "Recovering high dynamic range radiance maps from photographs," in *Proc. ACM SIGGRAPH97*, pp. 369–378, New York, Aug. 1997.

[25] C. Tomasi and R. Manduchi, "Bilateral filtering for gray and color images," in *Proc. IEEE Int. Conf. Computer Vision*, pp. 839–846, Bombay, India, Jan. 1998.

[26] D. J. Jobson, Z.-U. Rahman, and G. A. Woodell, "A multiscale Retinex for bridging the gap between color images and the human observation of scenes," *IEEE Trans. Image Processing*, vol. 6, no. 7, pp. 965–976, July 1997.

[27] R. Kimmel, M. Elad, D. Shaked, R. Keshet, and I. Sobel, "A variational framework for Retinex," *Int. Journal of Computer Vision*, vol. 52, no. 1, pp. 7–23. Apr. 2003.

[28] A. K. Jain, M. N. Murty, and P. J. Flynn, "Data clustering: A review," *ACM Computing Surveys*, vol. 31, no. 3, pp. 264–323, Sept. 1999.

[29] T. Kanungo, D. M. Mount, N. S. Netanyahu, C. D. Piatko, R. Silverman, and A. Y. Wu, "An efficient k-means clustering algorithm: Analysis and implementation," *IEEE Trans. Pattern Analysis and Machine Intelligence*, vol. 24, no. 7, pp. 881–892, July 2002.

[30] T.-H. Min, R.-H. Park, and S. Chang, "Histogram based ghost removal in high dynamic range images," in *Proc. IEEE Int. Conf. Multimedia and Expo ICME 2009*, pp. 530–533, New York, June/July 2009.

BIOGRAPHIES

Ji Won Lee received the B.S. degree in physics from Sookmyung Women's University in 1999. She received the B.S. and M.S. degrees in electronic engineering from Sogang University in 2004 and 2006, respectively. She is working toward the Ph.D. degree in electronic engineering at Sogang University. Her current research interests are image processing and resolution enhancement.

Rae-Hong Park (S'76-M'84-SM'99) was born in Seoul, Korea, in 1954. He received the B.S. and M.S. degrees in electronics engineering from Seoul National University, Seoul, Korea, in 1976 and 1979, respectively, and the M.S. and Ph.D. degrees in electrical engineering from Stanford University, Stanford, CA, in 1981 and 1984, respectively.

In 1984, he joined the faculty of the Department of Electronic Engineering, Sogang University, Seoul, Korea, where he is currently a Professor. In 1990, he spent his sabbatical year as a Visiting Associate Professor with the Computer Vision Laboratory, Center for Automation Research, University of Maryland at College Park. In 2001 and 2004, he spent sabbatical semesters at Digital Media Research and Development Center, Samsung Electronics Co., Ltd. (DTV image/video enhancement). His current research interests are video communication, computer vision, and pattern recognition. He served as Editor for the Korea Institute of Telematics and Electronics (KITE) Journal of Electronics Engineering from 1995 to 1996.

Dr. Park was the recipient of a 1990 Post-Doctoral Fellowship presented by the Korea Science and Engineering Foundation (KOSEF), the 1987 Academic Award presented by the KITE, the 2000 Haedong Paper Award presented by the Institute of Electronics Engineers of Korea (IEEK), the 1997 First Sogang Academic Award, and the 1999 Professor Achievement Excellence Award presented by Sogang University.

SoonKeun Chang received his B.S. degree in astronomy and space science from KyungHee University, Korea, in 2000 and M.S. degree in control engineering from Kanazawa University in 2003. He received a Ph.D. degree in control engineering from Tokyo Institute of Technology (TITech) in 2007. In 2007, he joined Samsung Techwin Co., Ltd., where he was involved in research and development of digital camera systems. Now he works at Samsung Electronics Co., Ltd., Korea. His main research interests include computer vision and image processing.